Microstructural Changes in Bitumen at the onset of Damage-healing

Nahar, Sayeda; Schmets, Alexander; Kasbergen, Cor; Schitter, G; Scarpas, Athanasios

Publication date
2016

Document Version
Final published version

Published in
CROW InfraDagen 2016

Microstructural Changes in Bitumen at the onset of Damage-healing

S.N. Nahar
Section of Pavement Engineering
Faculty of Civil Engineering & Geosciences, Delft University of Technology
Stevinweg 1, 2628 CN, Delft, The Netherlands.
Tel: +31(0)152789597, Fax: +31(0)152785767, E-Mail: s.n.nahar @tudelft.nl

A.J.M. Schmets[1], C. Kasbergen[1], G. Schitter[2] and A. Scarpas[1]
[1]Section of Pavement Engineering
Faculty of Civil Engineering & Geosciences, Delft University of Technology

[2]Automation and Control Institute (ACIN)
Vienna University of Technology

Abstract
Self-healing of bitumen is a property that positively contributes to the sustainability, maintenance requirements and cost effectiveness of asphalt pavements. Ideally one would like to design an asphalt mix with a well-defined healing potential. Although substantial research efforts have been dedicated to the healing mechanism in bitumen, complete understanding of the fundamental mechanisms that govern the property of healing is still lacking. Here we investigate the manifestation of damage and healing of bitumen at the microstructural level. Three distinct bitumen grades are subjected to mechanical loading conditions, and the damage is investigated at the microstructural level by atomic force microscopy combined with finite element simulations. One of the bituminous phases appears to display visible signs of cracks, which are found to (partly) disappear at moderate temperature changes. Simulations of mechanical loading of experimentally derived finite element meshes are corresponding well with these experimental observations. Moreover, the simulations provide a measure of mechanical response, i.e. stiffness, of the material as a function of strain level. From this it is found that the microstructural cracks lead to diminished structural response properties, whereas after healing these properties are partly recovered. The experimental observations, together with the simulations, support earlier ideas that relate the phenomenon of self-healing in bitumen to their rheological property of thixotropy. Moreover, the work presented hints that the property of self-healing is governed by processes at the microstructural length scale.

Keywords
bitumen, microstructure, Atomic Force Microscopy (AFM), micro-crack, thixotropy.

1. Introduction

An important and unique property of bituminous materials is their intrinsic ability to (partly) recover structural damage over time (*1-4*), usually termed as healing or self-healing. This healing property has been known for a long time, and it was originally introduced to bridge the difference between service life predictions based on laboratory (mechanical) tests and service life levels as observed in the field. Therefore, in the Netherlands during the 1970's a 'healing factor' of 4 was part of the pavement design guidelines. Nowadays such healing factor is not in practice anymore; nevertheless Dutch Road Authorities are interested in better understanding and quantification of the healing characteristics of their asphalt mixes; especially for reasons of sustainability, maintenance and costs.

From fatigue experiments aimed at mimicking healing of asphalt at laboratory conditions, it was found that the restoration, i.e. healing, recovery of strength and stiffness of bitumen is promoted by rest periods and by application of moderate amounts of heat (*3-8*). The healing process was described as a three stage process: crack closure followed by crack surface wetting and subsequent increase of adhesive force across (former) crack, driven by an (inter) diffusion mechanism (*1; 2; 9; 10*).

Other authors attribute the fatigue and healing characteristics of bitumen to the concept of thixotropy (*9-11*), which may actually be related to the mechanisms proposed in the previous paragraph. Thixotropy is the (constant) decrease of viscosity when a material that was initially at rest is forced to flow. The origin of this decrease in viscosity maybe attributed to the "breakdown and build-up of microstructure" (*10; 11*). This decrease of viscosity is, from the point of view of thixotropy, largely reversible, especially when strains remain below the fatigue endurance limit (*12*); from this perspective asphalt healing is nothing else than a reversible, rheological property of the binder, which requires longer timescales to develop (the rest periods in fatigue-healing tests). This justifies the study of damage and healing characteristics at microstructural length scales, where the breakdown and build-up of microstructure should be observable. Thus, in this study we investigate the hypothesis that thixotropic properties of bitumen are at the origin of the reversibility of damage in fatigue tests, by investigating the reversibility of microstructural changes in bitumen under mechanical loading.

The microstructure morphology of bitumen, i.e. its multiphase nature at room temperature, has been studied extensively over the past decade by utilizing new, advanced imaging techniques such as atomic force microscopy (AFM). In various studies researchers found evidence that microstructure provides a signature of chemical and physical properties of the material. The microstructure is found to vary with the source of the crude and is also found to correlate with fractions commonly mentioned in literature, like saturate and asphaltene fractions (*13; 14*). The morphology has also been related to mechanical, rheological and ageing characteristics of bitumen (*15; 16*).

Therefore, firstly the microstructure morphologies of three penetration (PEN) grade bitumen (10/20, 70/100 and 160/220), all obtained from the same crude oil source were imaged by AFM. The characteristic microstructure morphology suggests a correlation of bitumen grades to microstructural properties. Then, for the same bitumen, the damage and healing characteristics were studied. Therefore, a method has been developed to subject the samples to a uniform, displacement controlled mechanical load. The damage resulting from mechanical loading (up to 10% strain) was probed by AFM. It was found that damage in the form of micro-cracks predominantly occurred in one phase of the material's microstructure at the applied loading level. Similar damage behavior has been observed earlier for other

bitumen (*17; 18*), suggesting that the damage mechanism can be considered to be alike for various bitumen grades.

The same experiment was then simulated using the Finite Element Method (FEM), utilizing realistic mechanical property data as well as a mesh derived from an experimental microstructure observation. The same characteristic damage pattern was observed as for the load experiment. The force-displacement curve obtained shows a decrease of 'stiffness' with strain, as would be expected in the case of thixotropy (*10*).

Finally, the 'damaged specimen' were subjected to moderate amounts of heat (45 °C) for a short period of time in order to 'increase the kinetics' of a possible healing process. In countries with even moderate climates, such as the Netherlands, a pavement experiences such temperature many times per year. Examining the microstructure of these mildly treated samples showed the reversal of damage: regions of the sample that initially showed micro-cracks are apparently healed. The microstructure of the 'healed sample' looked very similar to the 'virgin' microstructure. Using the results from the FEM simulation, this would mean that also the macroscopic mechanical response of the material have been – complete or partially – recovered. By heating the damaged material even higher temperatures (90 °C) and subsequent cooling to room temperature, shows complete rearrangement of the microstructural properties, i.e. loss of memory of the previous microstructural state.

2. Objectives

The objectives of this study were to:

1. to study the effect of mechanical loading on the microstructural length scale, both experimentally and by simulation;
2. to study the effect of rest periods and application of moderate amounts of heat (to shorten rest period, provided time-temperature superposition is valid) on the mechanically loaded material;
3. to relate the experimental observations with the findings from macroscopic mechanical tests, claiming that the phenomenon of healing can (partly) be attributed to thixotropic effects (10; 12).

The added value of this research is that here a material property (microstructure) is being related to macroscopic mechanical test results. As healing is ultimately a material property, the long term goal of this research line would be to establish firm correlations between binder (microstructural) material properties, and mechanical characteristics like fatigue endurance limit of the same material as ingredient of a pavement structure. Better understanding of these correlations may give direction to developing materials with tailored healing characteristics.

2. Materials and methods

2.1 Materials

For comparing the microstructures of different grades, straight run bitumen with penetration grades of 10/20, 70/100 (PG58-28), 160/220 were selected. The materials were obtained from a single crude oil source, and were provided by Kuwait Petroleum International (Q8). Later,

two bitumen grades, 70/100 and 160/220 have been selected for investigating the crack morphology healing at the micro-level.

2.2 Methods

To measure the microstructure of the neat bitumen, samples were prepared on round steel substrates of 12 mm diameter (i.e. AFM sample puck). Each specimen was prepared by applying a bead of 20 mg bitumen sample to the substrate by a spatula and afterwards, the substrate was heated on a hot plate at 100 °C for 30 seconds. This results in a thin (0.3-0.4 mm), smooth film of bitumen that is suitable for AFM imaging. Next, the specimens were thermally conditioned inside an oven at 100 °C for 30 minutes followed by cooling in ambient air and equilibration at room temperature for 24 hours.

Another batch of specimens was prepared on a special substrate by following the aforementioned procedure. The substrate system consists of a piece of aluminium tape that is attached to the sample puck by its adhesive side. Here, aluminium tape was selected because of its favourable thermal conductivity property (at 25 °C, k = 205 $Wm^{-1}K^{-1}$). This guarantees optimal heat transfer between substrate and sample, which is especially important for the healing study. Then, the specimens were thermally conditioned in a convection oven by following the aforementioned procedure. The AFM measurement was performed after air cooling and equilibration of the specimen at room temperature for 24 hours.

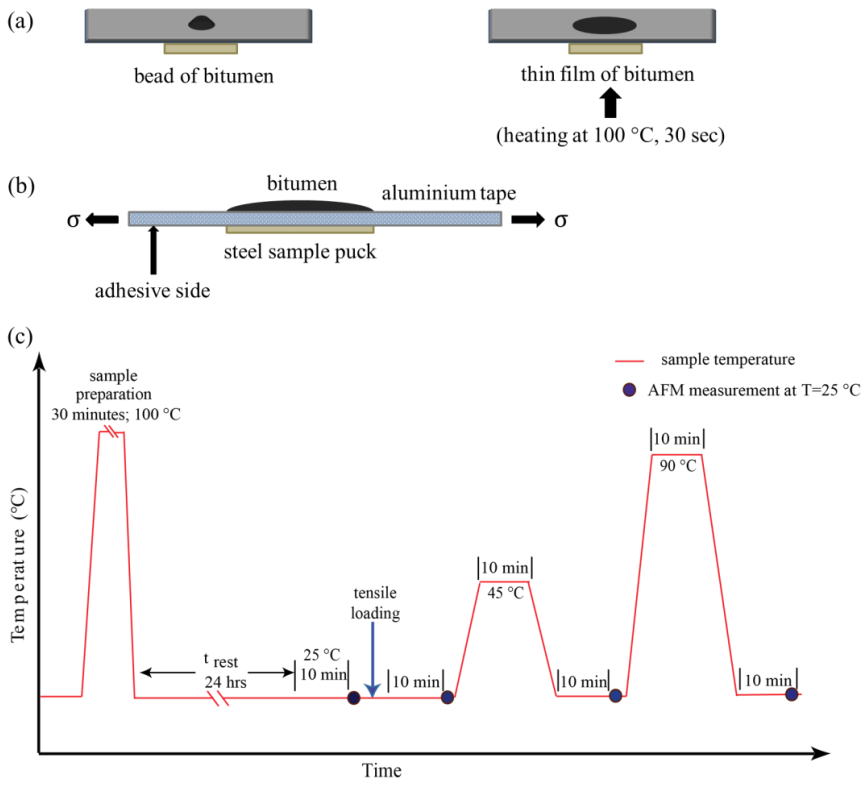

Figure 1: (a) Sample substrate system, (b) mechanical loading set-up, and (c) schematic representation of thermal conditioning of specimen and AFM imaging protocol.

Subsequently, the specimen was strained to 10% by pulling the tape from both sides along a ruler, Figure 1(b). The microstructure of the strained sample was measured by AFM after a rest period of 10 minutes as shown in Figure 1(c). Following that, the specimen was heated to 45 °C and cooled down to 25 °C in real-time, using the heated-cooler stage of the

AFM set-up. Microstructural changes were probed in situ with an equilibration time of 10 minutes. The specimen was heated again to 90 °C and cooled down to 25 °C. For every temperature step a similar equilibration time was used prior to AFM imaging. In order to guarantee repeatability of the experiments, the same preparation and measurement procedure were carried out on three samples per bitumen grade.

2.3 AFM instrumental settings

AFM images were taken in tapping mode using 'Multimode V' AFM-setup from Bruker (Santa Barbara, USA). During the second phase of the research, while operating the real-time thermal conditioning steps, the heater and cooler stage system with a modified version of the AS-130V scanner ('J' vertical) from Bruker were utilized. It enables to perform AFM imaging with precise temperature control of the sample, at broad range of temperatures (-35 to 250 ºC). The main components of the heater and cooler system include a platinum resistive type heating element, a special heater/cooler AFM scanner with a fluid heat exchanger, a thermal applications controller and a spacer block to allow the system to be operated with the special AFM scanner.

All AFM scans were performed using tapping mode in air at 25 °C. RTESP (Bruker), tapping mode silicon cantilevers (AFM probe) were used for all measurements. The nominal dimension of the cantilever was 120×35×3 μm^3. The force constant and resonant frequency of the cantilever was 40 N/m and 330 kHz respectively. The probe was scanned over the sample surface at scan rate of 1.0 Hz (1 line/s). Overview images were recorded at scan size of 30×30 μm^2 with a pixel resolution of 512×512 and the high resolution scans were obtained at 10×10 μm^2 with the same pixel resolutions. The offline AFM image analysis was performed using the Gwyddion software package (*19*).

3. Experimental results and discussion

3.1 Microstructure morphology of the undamaged bitumen

The first batch of specimens was used to determine the microstructure of the three bitumen prior to mechanical loading. The three specimens were prepared as described in the methods section. The microstructure of bitumen was imaged by tapping mode AFM. The recorded topography and phase images (30×30 μm^2) are presented in Figure 3, displaying the microstructure of the three respective bitumen at 25 °C. The phase images show typical two phase morphology for all bitumen studied, as has been observed for many other bitumen grades as well (*20-24*). The elliptical domains are designated as 'domain phase' and the continuous phase as 'matrix' phase. Both the topography and phase images show that domains of different morphology are dispersed in the matrix phase. The key observations of the microstructural properties are summarized in Table-1.

The microstructure of bitumen 10/20 is shown in Figure 2(a). In this bitumen, domains are observed to appear at the smallest size range of 0.3 to 0.6 µm and are found homogeneously distributed over the matrix phase. From the topography image of Figure 2 (a), it is confirmed that the domain phase of 10/20 doesn't show a 'wrinkling' pattern (i.e. topographical undulation), which is in agreement with earlier observations that below a certain domain size wrinkling does not appear (*16*). The topography image shows that all domains are 2 to 5 nm lower than the average height of the matrix phase, which is also a common observation (*18*). Besides, the domains appear mostly in clusters throughout this

bitumen. A comparable phase fraction of both phases is observed; the domain and matrix phases cover 47% and 53% of the surface area respectively (Table 1). Moreover, surface is extremely flat, with an average roughness of 0.6 nm and maximum height, z_{max}= 10 nm.

Table 1: Comparison of microstructural properties in bitumen of different PEN grades.

Microstructural feature	**Bitumen samples**		
	10/20	*70/100*	*160/220*
No. phases	2	2	2
Phase fraction			
Domain phase	47%	63%	47%
Matrix phase	53%	37%	53%
Characteristics of domain phase			
Appearance	agglomerated	occasional clustering	dispersed
Shape	round	elliptical	elliptical
Size range	0.3 to 0.6 µm	0.8 to 5.8 µm	0.8 to 9.5 µm
Wrinkling	absent	present	present
Average surface roughness	0.6 nm	2.9 nm	2.3 nm

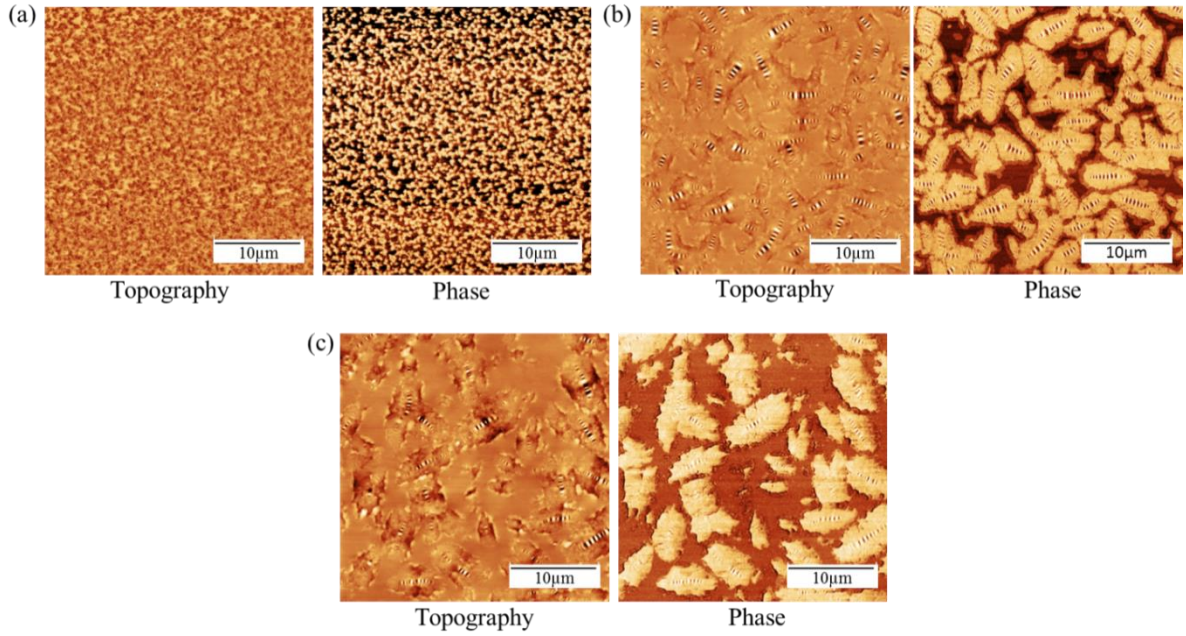

Figure 2: Microstructure of different PEN-grades of bitumen obtained from the same crude source. 30×30 µm^2 AFM topography and phase images of (a) 10/20 (b) 70/100 (c) 160/220.

The next bitumen grade, 70/100 is the type of grade commonly used in asphalt pavements in the Netherlands. The microstructure of this neat bitumen is shown in Figure 2(b). One observes the characteristic elongated domains with wrinkling pattern along the long axis and these domains are dispersed throughout the matrix phase. The size of the domain phase ranges from 0.8 to 5.8 µm. Besides, the domain phase also displays occasional clustering. Again, the domain and the matrix phases cover 63% and 37% of the surface area respectively. The topographical undulation (wrinkling) gives rise to a higher height range

(z_{max}= 90 nm) in the surface topology but as being localized, only contributes little to the average surface roughness of 2.9 nm (Table 1).

For the 160/220 grade, the microstructure displays the common appearance of wrinkled domains dispersed through a matrix, Figure 2(c). The microstructural properties are comparable to the 70/100 grade. There are mainly two size ranges of domains present. The lower size range has a lower abundance and ranges from 0.8 to 3 µm, while the upper range varies from 3 to 9.5 µm. Wrinkling is observed in most of the domains except some smaller domains (< 0.8 µm). Despite the presence of larger domains, the phase fraction of the domain phase is 47 % which is smaller than for the 70/100. The localized topographical undulations along the long axes of the domains contribute to a maximum height z_{max} of 65 nm. This also results in an average roughness of 2.3 nm over the scanned surface.

3.2 Load-induced micro-crack morphology and healing

Two bitumen grades, 70/100 and 160/220, were selected for the mechanical loading experiments. Damage in the other bitumen, 10/20, having a very fine-grained microstructure, may not be observable with the spatial resolution. The application of tensile load to the specimen was performed as shown in Figure 1(b). The tape substrate was strained (~10%) in a unidirectional and uniform fashion. This strain was also transferred to the bitumen film adhered to it, as could be observed from the shape change of the bitumen drop.

Next, the material was allowed to heal by application of heat, i.e. by in situ heating of the specimen to 45°C on the heater stage of the AFM set-up, followed by 10 minutes of equilibration time. The specimen was then cooled back to 25 °C and imaged again after 10 minutes. Finally, the specimen was heated to 90 °C and it was cooled to 25 °C after holding for 10 minutes at the set temperature. Then, after 10 minutes of rest time at the measuring temperature of 25 °C, the sample was measured again, Figure 1(c).

3.2.1 Experimental characterization of load-induced damage

The changes in microstructure of bitumen grades 70/100 and 160/220 after mechanical loading were measured in situ by AFM. Both the topography and phase images of the bitumen microstructure show evidence that the domain phase is the first to show signs of damage, though overall the two phase morphology of the neat bitumen is preserved. Only the phase images are presented here in Figure 4, as these images display the contours of the two phases most clearly throughout the microstructure. The representative AFM images of the strained bitumen films are shown as 30×30 µm^2 phase images, Figure 3 a(i)-b(i), while the direction of loading is indicated by an arrow. The precise damage characteristics (crack morphology) are presented in more detail in the 10×10 µm^2 phase images. A crack pattern is clearly present in the domains, whereas no signs of damage are observed throughout the matrix at this loading level. Cracks are mostly found oriented perpendicular to the long axes of the domains. Moreover, the orientation of the domains relative to the loading direction seemingly influences the damage and appearance of the crack pattern in the domains.

Some cracks are observed to propagate throughout the domains (continuous cracks), while other, tinier cracks (widths of 20 to 80 nm) end within the domain boundaries. These tiny cracks are designated as crazes.

At the location of the cracks and crazes one can observe, from the phase images, the matrix phase protruding. The matrix is a few nanometers (2 to 5 nm) higher in topography compared to the domains. From the topography images one observes that at the location of cracks the topography is also 2-5 nm higher, which confirms the protrusion of the matrix phase through the cracks in the domains. This indicates that the features that look like cracks

in the phase images are also discontinuities in topography. These observations have been more extensively reported elsewhere (*18*). In the 70/100 bitumen crack widths vary from 20 nm to 170 nm, whereas crack widths in 160/220 bitumen are in the range of 30 nm to 1.5 µm. The continuous cracks cause the domains of both the bitumen to break down into fragments. In the case of the 160/220 bitumen these fragments tend to dislocate.

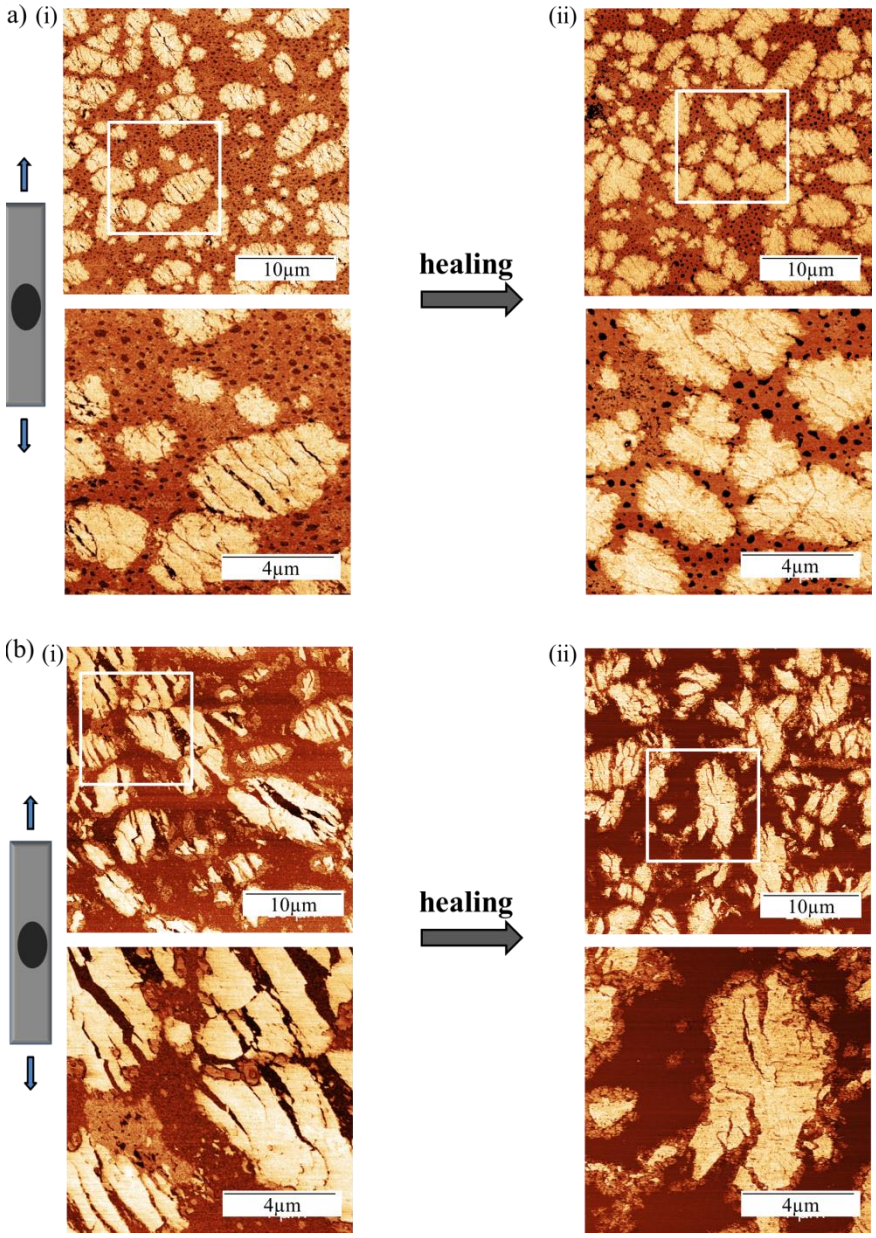

Figure 3: AFM phase images of bitumen microstructure at 25 °C a) 70/100 and (b) 160/220. 30×30 µm² overview and 10×10 µm² high resolution images of (i) microstructural changes after tensile loading and (ii) after moderate heating at 45 °C (healing or crack closure).

3.2.2 Simulation of load-induced damage

The same experiment as presented in the previous section has been simulated by the Finite Element Method (FEM). A typical 30×30 µm² AFM bitumen phase image was digitally processed into finite element meshes consisting of two material types for the phases, using

Simpleware software code, Figure 5a. The mesh was 3D, though there is a plane of symmetry at the middle (thickness direction) of the slab. The FEM simulation was a 3D simulation.

Then a viscoelastic Zener material model (*25*) which consists of two parallel components, an elastic spring and a Maxwell component, has been utilized for constitutive modelling. Additionally the standard model has been extended to include damage simulation. To allow for damage the second Piola-Kirchhoff stress S in the reference configuration is modified as $S_{eff} = (1-d)S$, where *d* is the damage parameter which can take values between '*0*' (no damage) and '*1*' (maximum damage). In this implementation the damage parameter *d* is a function of the total work *W* in the Zener component, $d = 1 - e^{-kW^r}$, with parameters *k* and *r*. Details about the simulations, such as boundary conditions, are provided elsewhere (*26*).

This model is then implemented within the finite element framework CAPA-3D (*25*) to simulate the response of bitumen to a monotonic, displacement controlled uniaxial loading in the y-direction, Figure 4(a). Material parameters like relaxation modulus E were derived from values obtained by dynamic shear rheometer (DSR) tests: the overall (averaged) parameters correspond to the DSR-derived values, whereas the range of properties 'per phase' were estimated from quantitative AFM measurements, e.g. (*14*). The values of the viscosity are based on a set of repeated simulations, varying this value. It should be emphasized that the precise value of the viscosity of the individual phases could not be measured, and represents an 'educated guess'. This has led to utilize an elastic modulus of 220 MPa for the domains and 150 MPa for the continuous phase. In Figure 1b-e the development of damage at intermediate strain states between 2-10% is shown 'on top of' the microstructure, allowing monitoring the localisation of damage during loading.

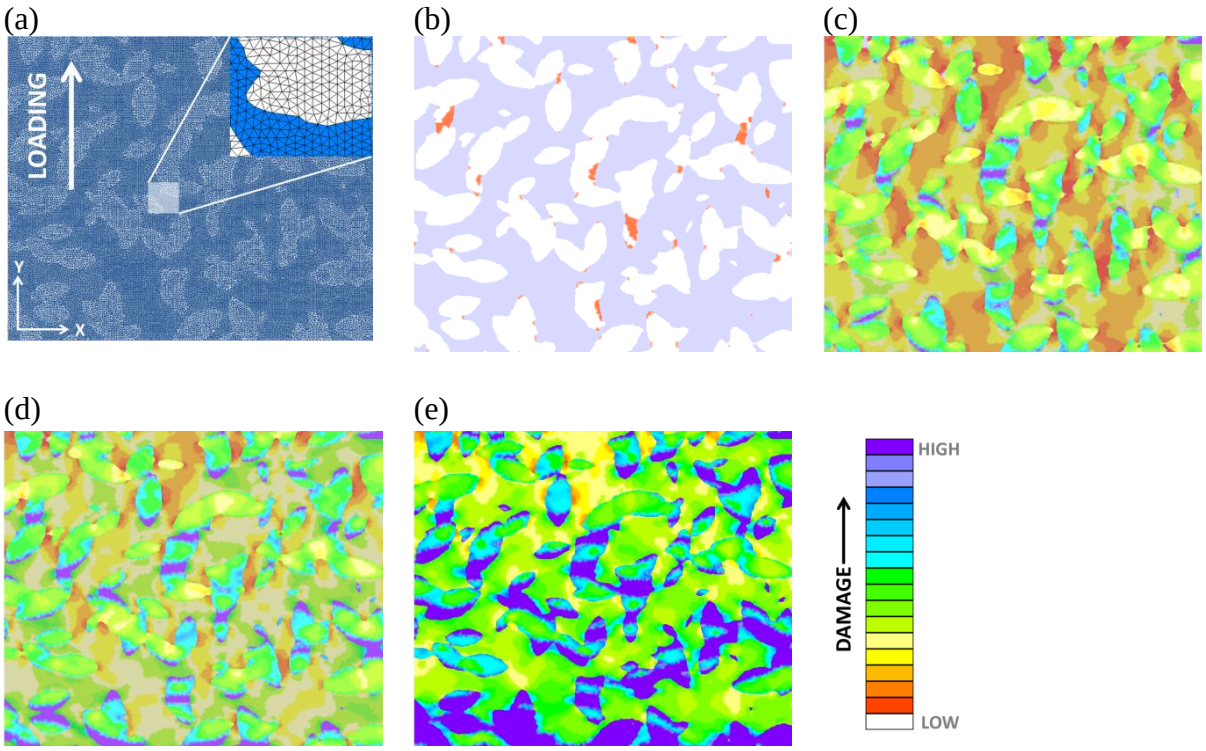

Figure 4: Finite element simulation of monotonic, displacement controlled loading with a strain rate of 0.02 s^{-1} in y-direction. (a) Finite element mesh from processing 30×30 μm^2 AFM phase image, for intermediate strain states of (b) 2%, (c), 4%, (d) 6% and (e) 10%.

The results of the FEM simulation, Figure 4, correspond well with the main observations made with AFM. At the application of loading damage initiates predominantly in the domains, close to the phase boundaries. At higher strain levels 'regions of high damage' occur throughout the domains, resembling the 'continuous cracks' throughout the domains as observed by AFM. The 'cracks' in the simulation also tend to be perpendicular to the long axes of the domains. Moreover, the amount of damage in a domain correlates to the orientation of the domain axis with respect to the loading direction: domains oriented parallel to the direction of loading show higher damage levels, with damage patterns perpendicular to the loading direction.

In Figure 5 the full response of the material to straining is presented in a force-displacement curve. One observes that the material displays yielding at about 12% strain. The tangent to the force-displacement curve decreases with strain level. i.e. the apparent stiffness (the tangent is a measure for the modulus) decreases with strain level. This behaviour can be associated with the aforementioned phenomenon of thixotropy. Also the assumption that thixotropy originates from a "breakdown and build-up of microstructure" (*10*), is supported by the FEM simulation: the insets in Figure 6, as well as the experimental observations in Figure 4, show damage in the form of fragmenting of domains at increased strain levels.

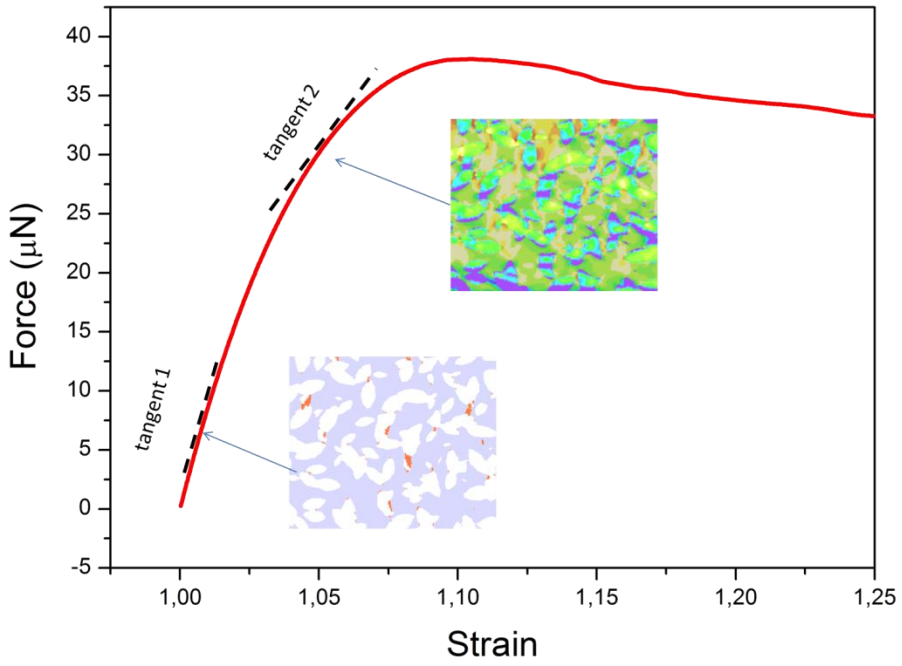

Figure 5: Force-displacement curve obtained from FEM simulations of monotonic loading of a bitumen-derived finite element mesh.

3.2.3 Observation of damage reversal and healing

Both samples that were previously subjected to mechanical loading, were then moderately heated (at 45 °C) and the microstructural changes were subsequently recorded at 25 °C. The AFM phase images of both samples are shown in Figure 3a (ii) and 3b (ii). Here both the overview ($30\times30\mu m^2$) and high resolution ($10\times10\mu m^2$) images reveal the details of the microstructural changes: the microstructural properties of the original, not strained bitumen does almost completely reappear. That is, we observe healing of damage at the microstructural level. Moreover, from these images one can infer that the microstructural

recovery of the 70/100 bitumen is more complete than for the 160/220 bitumen. Apparently, given the experimental conditions, the 70/100 has the favorable healing characteristics.

3.2.4 Damage reversal and healing by total morphological memory erasure

The microstructural properties of the strained bitumen can be replenished, if the micro-cracks and crazes of the microstructure can be completely removed. This can be achieved by invoking a complete rearrangement of the microstructure of the strained specimens. To achieve this, the specimens from both bitumen were heated to 90 °C that were formerly tensile loaded and were exposed to moderate heat as shown in Figure 2. The microstructural changes were measured by AFM after cooling down from 90 °C to 25 °C. AFM topography and phase images of 30×30μm^2 and high resolution 10×10μm^2 images of 70/100 and 160/220 are shown in Figure 6(a) and Figure 6(b) respectively. Heating the specimen to this temperature (90 °C) causes melting of the domains and turns the material to a single continuous phase (*13*). By subsequent cooling from its melt, the domain phase starts to nucleate within the matrix phase. The characteristic morphology of the microstructure is fully developed at temperatures close to 25°C. The AFM measurements presented in Figure 7, exhibit no traces of cracks or crazes anymore; a new microstructure morphology appears, which differs from that of the neat bitumen as observed in Figure 3 but show the characteristic main features of the microstructure .

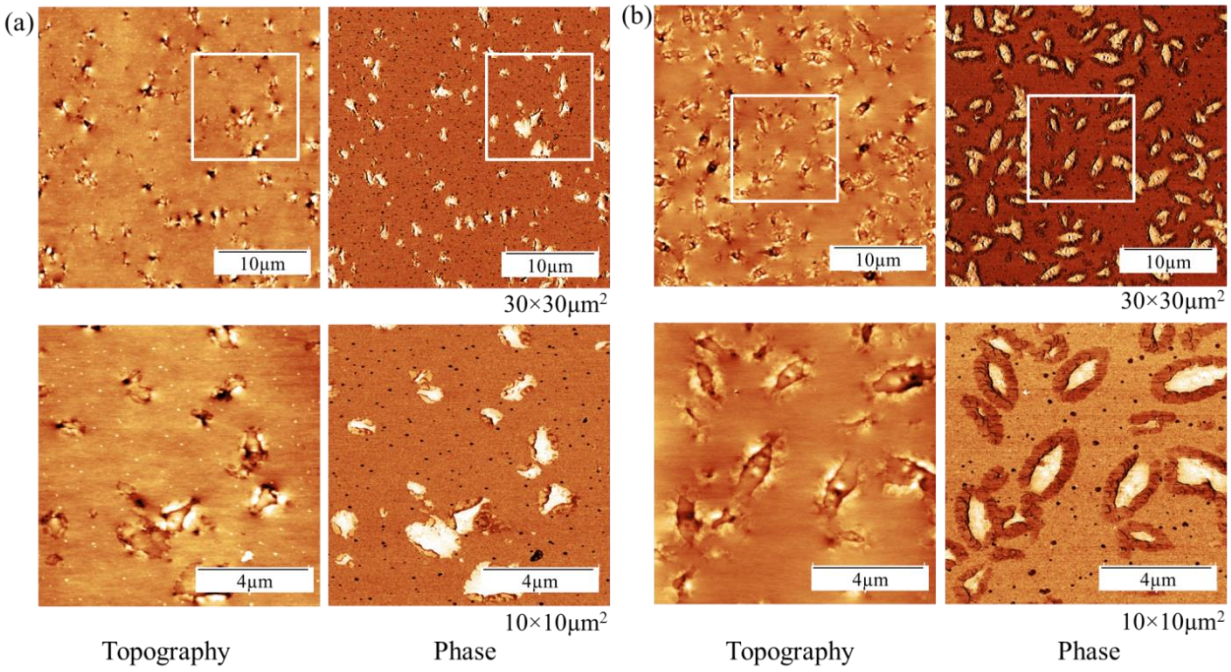

Figure 6: AFM topography and phase images of bitumen microstructure, captured at 25 °C after cooling from 90 °C to 25 °C. 30×30 μm^2 overview and 10×10 μm^2 zoomed in images of a) 70/100 and (b) 160/220.

4. Conclusions

The microstructure of three penetration grades bitumen from a single crude source was measured by AFM. All bitumen exhibit the characteristic two-phase morphology. The hardest grade (10/20) shows a homogeneous microstructure where the domain phase appears in very small size and without any topographical undulation. The microstructural morphology of this bitumen grade is quite comparable to the field aged bitumen (*15*). The second bitumen grade, 70/100, also displays the typical microstructural properties of bitumen. In this bitumen, topographical undulations are observed along the long axis of the elliptical domain. The softest bitumen, 160/220 exhibits the largest domains. Hence, in agreement with literature findings, it can be concluded that penetration grade correlates with the size of the domains (*13; 15; 16*); domain sizes are larger for softer grades.

The influence of unidirectional, monotonic mechanical loading at the microstructural level was shown for two bitumen grades (70/100 and 160/220). Micro-cracks leading to the fragmentation of the domain phase were observed in both bitumen. The crack morphology may vary depending on the microstructural properties of bitumen and the loading level. As the bitumen of different penetration grades exhibit varied microstructural properties, crack characteristics (such as widths) were also found to different for a same level of loading.

A similar loading scenario has been simulated using FEM on an experimentally derived finite element mesh, and using experimental values for the mechanical properties of the phases. The simulated response to strain resembled closely the findings obtained by AFM: damage predominantly occurs in the domains, leading to continuous areas of 'high damage' throughout the domains, associated with (continuous) cracks. From the simulated force-displacement curve a decrease of stiffness with level of strain is observed. This is comparable to the phenomenon of thixotropy.

Application of moderate heat (45 °C) to the strained specimen led to disappearance of most of the features that were associated with cracks, and the original microstructure was (partly) recovered. That is: healing was observed at the microstructural length scale. From the FEM simulations it can be inferred that the disappearance of cracks will be accompanied by an increase in stiffness; the structural response will be similar to that of a material with less cracks or fragments. This in agreement with the statement that thixotropy relates to changes at the microstructural level. Although this provides evidence that thixotropy, and the underlying kinetic processes governing it, is related to healing, other mechanisms leading to healing such as crack surface wetting followed by inter-diffusion (*3; 5*) cannot be ruled out. Both mechanisms may actually be the same, though observed at different length scales. In this study, the healing potential of the harder bitumen is found to be higher than that of the softer grade (a larger range of similar experiments is needed to generalize this statement to all binders). A possible explanation for this is that smaller crack widths, as present in the harder bitumen, can heal more easily. Further heating of the material to its melt (single phase) and successive cooling leads to complete memory erasure, all (micro) cracks disappear, and a new microstructure morphology emerges.

Thus, here we presented the effect of mechanical loading at the microstructural length scale by imaging the characteristics of mechanical damage. Damage was observed as cracks in the domain phase. Damage could be (partially) reversed by applying moderate thermal conditions: the domain cracks tend to disappear. Simulations showed that the disappearance of cracks will be accompanied by an increase of structural response characteristics of the material, such as stiffness. The observations from experiment and simulations are in support of earlier studies that relate the healing behavior of bituminous materials to thixotropy. Further experiments, rheology in combination with microstructural studies, may be carried out

to further clarify the relation between microstructure, thixotropic and healing properties of bitumen. Once this relation is established, one could think of designing bitumen grades with desired healing properties.

Acknowledgement

We acknowledge Jeroen Besamusca from Kuwait Petroleum Research & Technology for providing the bitumen. This work builds on work previous work done in collaboration with Troy Pauli, Western Research Institute. Financial support from the national IOP Self-Healing Materials program (Netherlands Enterprise Agency, the Hague, the Netherlands) under grant no. SHM01056 is gratefully acknowledged.

References

[1] Kim, Y. R., and D. N. Little. Evaluation of healing in asphalt concrete by means of the theory of nonlinear viscoelasticity. *Transportation Research Record*, No. 1228, 1989.
[2] Kim, Y.-R., D. Little, and R. Lytton. Evaluation of Microdamage, Healing, and Heat Dissipation of Asphalt Mixtures, Using a Dynamic Mechanical Analyzer. *Transportation Research Record: Journal of the Transportation Research Board*, Vol. 1767, No. -1, 2001, pp. 60-66.
[3] Little, D., and A. Bhasin. Exploring Mechanism of H ealing in Asphalt Mixtures and Quantifying its Impact.In *Self Healing Materials, No. 100*, Springer Netherlands, 2007. pp. 205-218.
[4] Little, D. N., R. Lytton, D. Williams, and C. Chen. Microdamage healing in asphalt and asphalt concrete, volume I: microdamage and microdamage healing, project summary report.In, 2001.
[5] Bhasin, A., D. N. Little, R. Bommavaram, and K. Vasconcelos. A Framework to Quantify the Effect of Healing in Bituminous Materials using Material Properties. *Road Materials and Pavement Design*, Vol. 9, No. sup1, 2008, pp. 219-242.
[6] Jones, I., and T. Kennedy. Asphalt chemistry and its effect on roadway surface conditions. *ASTM Standardization News*, Vol. 19, No. 2, 1991.
[7] Kringos, N., A. Scarpas, T. Pauli, and R. Robertson. A thermodynamic approach to healing in bitumen. *Advanced testing and characterization of bituminous materials*, 2010, pp. 123-128.
[8] Qiu, J., M. F. C. van de Ven, S. Wu, J. Yu, and A. A. A. Molenaar. Investigating the Self Healing Capability of Bituminous Binders. *Road Materials and Pavement Design*, Vol. 10, No. sup1, 2009, pp. 81-94.
[9] Pronk, A. C. PH Model in 4PB Tests with Rest Periods. *Road Materials and Pavement Design*, Vol. 10, No. 2, 2009, pp. 417-426.
[10] Shan, L., Y. Tan, S. Underwood, and Y. Kim. Application of Thixotropy to Analyze Fatigue and Healing Characteristics of Asphalt Binder. *Transportation Research Record: Journal of the Transportation Research Board*, Vol. 2179, No. -1, 2010, pp. 85-92.
[11] Pérez-Jiménez, F., R. Botella, and R. Miró. Damage and Thixotropy in Asphalt Mixture and Binder Fatigue Tests. *Transportation Research Record: Journal of the Transportation Research Board*, Vol. 2293, No. -1, 2012, pp. 8-17.
[12] Zeiada, W., M. Souliman, K. Kaloush, and M. Mamlouk. Endurance Limit for HMA Based on Healing Concept Using Uniaxial Tension-Compression Fatigue Test. *Journal of Materials in Civil Engineering*, Vol. 26, No. 8, 2013, p. 04014036.
[13] Nahar, S. N., A. J. M. Schmets, A. Scarpas, and G. Schitter. Temperature and thermal history dependence of the microstructure in bituminous materials. *European Polymer Journal*, Vol. 49, No. 8, 2013, pp. 1964-1974.
[14] Nahar, S. N., A. J. M. Schmets, G. Schitter, and A. Scarpas. Quantitative Nanomechanical Property Mapping of Bitumen Micro-Phases by Peak-Force Atomic Force Microscopy.In *12th ISAP Conference on Asphalt Pavements*, Raleigh, North Carolina, USA, 2014.

[15] Nahar, S., M. Mohajeri, A. Schmets, A. Scarpas, M. van de Ven, and G. Schitter. First Observation of Blending-Zone Morphology at Interface of Reclaimed Asphalt Binder and Virgin Bitumen. *Transportation Research Record: Journal of the Transportation Research Board*, Vol. 2370, No. -1, 2013, pp. 1-9.
[16] Nahar, S. N., J. Qiu, A. J. M. Schmets, E. Schlangen, M. Shirazi, M. F. C. van de Ven, G. Schitter, and A. Scarpas. Turning back time: Rheological and microstructural assessment of rejuvenated bitumen. *TRB 93rd Annual Meeting Compendium of Papers*, 2014, pp. 1-17.
[17] Nahar, S. N., A. J. M. Schmets, A. Scarpas, and G. Schitter. Temperature induced healing in strained bituminous materials observed by atomic force microscopy.In *Fourth International Conference on Self-Healing Materials*, Magnel Laboratory for Concrete Research Ghent, Belgium, 2013. p. 220.
[18] Nahar, S. N., A. J. M. Schmets, A. Scarpas, and G. Schitter. Microstructural changes in bitumen at the onset of crack formation. *European Polymer Journal*, Vol. 56, No. 0, 2014, pp. 17-25.
[19] Klapetek, P., D. Necas, and C. Anderson. *Gwyddion user guide*. 2008.
[20] Masson, J. F., V. Leblond, and J. Margeson. Bitumen morphologies by phase-detection atomic force microscopy. *Journal of Microscopy*, Vol. 221, No. 1, 2006, pp. 17-29.
[21] Masson, J. F., V. Leblond, J. Margeson, and S. Bundalo-Perc. Low-temperature bitumen stiffness and viscous paraffinic nano- and micro-domains by cryogenic AFM and PDM. *Journal of Microscopy*, Vol. 227, No. 3, 2007, pp. 191-202.
[22] Pauli, A. T., J. F. Branthaver, C. M. Eggleston, and W. Grimes. Atomic force microscopy investigation of SHRP asphalts. *Abstracts of Papers of the American Chemical Society*, Vol. 221, 2001, pp. U220-U220.
[23] Pauli, A. T., R. W. Grimes, A. G. Beemer, T. F. Turner, and J. F. Branthaver. Morphology of asphalts, asphalt fractions and model wax-doped asphalts studied by atomic force microscopy. *International Journal of Pavement Engineering*, Vol. 12, No. 4, 2011, pp. 291-309.
[24] Schmets, A., N. Kringos, T. Pauli, P. Redelius, and T. Scarpas. On the existence of wax-induced phase separation in bitumen. *International Journal of Pavement Engineering*, Vol. 11, No. 6, 2010, pp. 555-563.
[25] Scarpas, A. *A Mechanics based computational platform for pavement engineering.* Delft University of Technology, Delft, Netherlands2005.
[26] Pauli, A. T., A. J. M. Schmets, C. Kasbergen, and A. Scarpas. Chemomechanical Modeling of Damage and Damage Recovery in Bituminous Asphalt Binders via a Micro-Finite Element Platform. *In preparation*.